Highly Stable Phospholipid Unilamellar Vesicles from Spontaneous Vesiculation: A DLS and SANS Study

Baohua Yue,[†] Chien-Yueh Huang,*[,†] Mu-Ping Nieh,[‡,§] Charles J. Glinka,[||] and John Katsaras[‡]

Otto H. York Department of Chemical Engineering and Department of Chemistry and Environmental Science, New Jersey Institute of Technology, Newark, New Jersey 07102, National Research Council, Steacie Institute for Molecular Sciences, Chalk River, Ontario K0J 1J0, Canada, Department of Physics, University of Guelph, Guelph, Ontario N1G-2W1, Canada, and Center for Neutron Research, National Institute of Standards and Technology, Gaithersburg, Maryland 20899

Received: June 9, 2004; In Final Form: September 8, 2004

Spontaneously formed unilamellar vesicles (ULV) composed of short- and long-chain phospholipids, dihexanoyl phosphorylcholine (DHPC) and dimyristoyl phosphorylcholine (DMPC), respectively, were doped with a negatively charged lipid, dimyristoyl phosphorylglycerol (DMPG), and studied with small-angle neutron scattering (SANS) and dynamic light scattering (DLS). Upon dilution, the spontaneous formation of vesicles was found to take place from bilayered micelles, or so-called "bicelles". SANS and DLS data show that ULV with narrow size distributions are highly stable at low lipid (C_{lp} < 0.50 wt %) and NaCl salt (C_s) concentrations. ULV size was found to be independent of both C_{lp} and C_s when they were below 0.33 and 0.5 wt %, respectively. Surface charge and salinity were found to be important factors in preparing ULV of a certain size. This observation is not in complete agreement with previous experimental results and cannot be completely explained with current theoretical predictions based on equilibrium calculations for catanionic surfactant mixtures. ULV size is found to be invariant over a wide range of temperatures, both below and above the phase-transition temperature, T_M, of DMPC, and was stable for periods of weeks and months, even after sonication.

Introduction

Unilamellar vesicles (ULV) consisting of a single closed bilayer are considered to be one of the better drug encapsulation and delivery devices. Although liposomal ULV often form spontaneously in vivo, they are seldom found in simple aqueous solutions. Over the past decade, several groups have investigated spontaneously forming ULV occurring in certain cationic−anionic surfactant[1−12] and cationic surfactant systems.[13] However, because of biocompatibility issues, surfactant systems are normally considered to be less suitable for biological applications.

Conventional methods for the preparation of lipid ULV are tedious and involve procedures such as repeated freezing and thawing, multiple extrusions, and sonications. Normally, high pressure is required to produce small, extruded ULV (pore size ∼50 nm or smaller), and the production rate is very low. Another concern of extruded vesicles is that the samples are almost always contaminated with larger multilamellar vesicles (MLV). In contrast, spontaneous forming ULV have many advantages, including ease of preparation, good size reproducibility, high stability over time, and less contamination from MLV. Because these ULV are formed "spontaneously", they can either be energetically stable or kinetically trapped. For the purposes of drug delivery, of great interest are their low polydispersity and size (50−150 nm).[14,15] Here, we report on the characteristics of spontaneously forming, stable phospholipid ULV. Their size and polydispersity and the insensitivity of these two characteristics to changes in lipid concentration and salinity make them likely candidates as drug-delivery vehicles.

Spontaneously forming ULV were previously observed in solutions consisting of long- and short-chain lipid mixtures.[16,17] Typically, they were obtained from micelle-to-vesicle transitions induced by detergent elimination[18−20] or a temperature jump.[21−24] In those studies, the average vesicle radius, $\langle R_o \rangle$, was always found to change with lipid concentration, C_{lp}, indicating that the ULV were sensitive to the chemical potential of the lipids. A recent study[25,26] has shown that the structure and size of spontaneously forming DMPG or Ca^{2+}-doped ULV were practically independent over a wide range of C_{lp}. However, when the systems were doped with both DMPG and Ca^{2+}, vesicle radius again became sensitive to changes in C_{lp}. It is known that adding Ca^{2+} to lipid mixtures alters the ionic strength of the solution and the bilayer's charge density because of the strong chemical binding of Ca^{2+} ions with PC headgroups.[27] In the present study, we attempt to minimize these complications by using NaCl, instead of $CaCl_2$, as Na^+ does not bind with the lipid headgroups as strongly as Ca^{2+} but instead forms a "loose" counterion layer surrounding the headgroups, as previously revealed by NMR.[27,28]

Most theoretical studies of spontaneous vesiculation and ULV stability were applied to equilibrium systems. Using Helfrich's model[29] and fluid lipid bilayers, the microscopic energy per spherical vesicle has a simple scale-free relationship of $4\pi(2k_b + k_G)$, where k_b and k_G are the bending modulus and Gaussian modulus, respectively. These moduli depend on factors such as surfactant distribution, cosurfactants, surface charge, molecule packing, and so forth. Winterhalter and Helfrich[30,31] and other

* Corresponding author. E-mail: mhuang@adm.njit.edu.
[†] New Jersey Institute of Technology.
[‡] Steacie Institute for Molecular Sciences.
[§] University of Guelph.
[||] National Institute of Standards and Technology.

10.1021/jp047510q CCC: $30.25
Published on Web 12/16/2004

groups[32−35] have examined the effect of electrostatic double layers on the bending elasticity of fluid membranes using Poisson−Boltzmann (P-B) theory. One of the most prominent findings is that the Gaussian modulus, depending on charge density and the Debye length, can be negative for the spontaneous formation of ULV. Safran et al.[36,37] calculated the free energy of ULV formed in surfactant mixtures and suggested that, compared to extended lamellae, surfactant mixtures with a high bending modulus may yield a lower elastic energy if there is a strong attraction between the two surfactants. Bergström and Eriksson[8,9] derived an effective k_b for surfactant mixtures by considering a variety of contributions such as geometric packing, Coulombic and headgroup interactions, chain conformation, and mixing. Oberdisse et al.[38−40] applied the so-called vesicle cell model (VCM) and P-B theory to investigate the effect of charge density (ρ), dilution, salinity, and bending modulus on ULV size. Israelachvili et al.[41,42] developed mean-field theories by considering molecular geometric packing, self-assembly, and interactions among surfactant molecules and lipids. More sophisticated molecular models,[43−45] which consider the energy change related to molecular translation and rotation, headgroup interaction, chain conformation, and electrostatic interactions, have also been employed to predict the size of small ULV.

It has recently been reported[18−20,45] that spontaneously forming ULV may be kinetically trapped. These findings led to the kinetic model proposed by Leng et al.,[46,47] which suggests a growth mechanism for bicelles upon dilution and the closure of large bicelles to form vesicles when the perimeter line tension dominates the bending elastic energy. The size of the kinetically trapped vesicles can thus be determined by controlling C_{lp} and C_s.

The present work investigates the self-assembled structures of DMPC/DMPG/DHPC mixtures doped with Na^+ using SANS and DLS. Surface charge is introduced by doping with the negatively charged lipid, DMPG. Compared to Ca^{2+}, Na^+ does not bind tenaciously to lipid headgroups, thus the surface charge density of Na^+-doped mixtures can simply be controlled with the DMPG/DMPC molar ratio. Nevertheless, it is noticed that the zeta potential of the vesicles may be affected by the electrochemical double layer and thus the concentration of NaCl.[27,28] The vesicle size was monitored as a function of lipid concentration (C_{lp}), solution salinity (C_s), temperature (T), and time (t). Throughout the experiment, the molar ratio of long- (DMPC) to short-chain (DHPC) lipids remained constant at 4.0, whereas the DMPC/DMPG ratio for all samples was 60. These molar ratios were selected on the basis of our previous experimental results (data not shown), which indicate that stable ULV exist only for DMPC/DHPC molar ratios between 2 and 5. Beyond this range, DMPC/DHPC/DMPG mixtures form discoidal bicelles or MLV.[23−26]

A structural phase diagram of lipid mixtures in the dilute regime (C_{lp} < 1.00 wt %) is presented. It is found that under numerous experimental conditions the ULV size is insensitive to both C_{lp} and C_s. The structural phase diagram is consistent with Winterhalter and Helfrich's prediction,[31] namely, that at the surface charge densities and Debye lengths studied, the calculated Gaussian modulus and total elastic energy are negative, predicting the spontaneous formation of ULV. As salinity increases, the total elastic energy increases, eventually leading to a ULV−MLV transition. The origin of nearly constant-size vesicles as a function of lipid concentration and salinity is presently not clear: at low C_{lp}, it may be due to the dominant role of enthalpic interactions or due to kinetic reasons during ULV formation. Despite this lack of detailed understanding, the DLS results are highly reproducible, and most samples remained unchanged for weeks and even months at low C_{lp}. Strong mechanical energy input, such as vortexing, centrifugation, and even bath sonication, was applied to the ULV, but no size change was observed once they were formed.

Experimental Section

Materials. DMPC, DHPC, and DMPG were purchased from Avanti Polar Lipids[54] (Alabaster, AL); sodium chloride (NaCl) was obtained from Sigma-Aldrich (St. Louis, MO). All chemicals were used as received. Prior to use, deuterium oxide (99.8%, Fisher Scientific) was filtered through a 0.1-μm Millipore Millex-VV sterile syringe-driven PVDF filter.

Sample Preparation. Stock solutions of DMPC/DHPC (molar ratio = 4/1) and DMPC/DMPG/DHPC (molar ratio = 60/2/15) were prepared to a C_{lp} of 5.00 wt % in D_2O. Vortexing and temperature cycling from 4 to 50 °C were used to dissolve the lipids. The two 5.00 wt % solutions were then mixed accordingly to a final DMPC/DMPG/DHPC molar ratio of 60/1/15. After equilibrating for 24 h at T = 4 °C, the solutions were diluted to C_{lp} = 1.00 wt % using filtered D_2O. Sodium chloride was then added to yield a C_s in the range of 0.10 to 1.00%. The solutions were then frozen at −10 °C followed by a single thawing step to room temperature for better mixing. Finally, solutions were diluted with appropriate amounts of D_2O to the final C_{lp} values. After preparation, samples were stored at 4 °C for 4 months, and selected samples were further incubated at 30 °C for a period of 1 month. Most samples were occasionally tested using DLS over the 5-month period, whereas all SANS experiments were conducted 1 month after sample preparation.

Small-Angle Neutron Scattering

Theory. The scattering intensity, $I(\mathbf{Q})$, from a solution composed of particles can be expressed in terms of a form factor, $F(\mathbf{Q})$, and a structure factor, $S(\mathbf{Q})$, where $\mathbf{Q}$ is the scattering vector ($\mathbf{Q} = (4\pi/\lambda)\sin(\theta/2)$). The form factor reveals the geometric characteristics of the single aggregate in solution, and the structure factor accounts for correlations due to interparticle interactions. The form factor and the structure factor are assumed to be independent, and the scattering intensity can be expressed as

$$I(\mathbf{Q}) \propto n_p |\langle F(\mathbf{Q})\rangle|^2 S(\mathbf{Q}) \quad (1)$$

where n_p is the number density of the scattering particles.

In our case, the $F(\mathbf{Q})$ of a ULV can be simulated using a spherical shell model with three parameters: vesicle size, bilayer (shell) thickness, and polydispersity.[23,24,26] For $S(\mathbf{Q})$, an analytical form can be obtained by solving the Ornstein−Zernike equation using a mean spherical approximation (MSA).[48] The derived $S(\mathbf{Q})$, which accounts for the repulsive electrostatic interactions between particles, was used in fitting the ULV system. The parameters pertaining to ULV charge density and salt concentration can be estimated from C_{lp} and C_s; a 20% variation is allowed in the fitting procedure.

Experiment. SANS experiments were conducted using the 30m NG7 SANS (Glinka et al., 1998) located at the NIST Center for Neutron Research (Gaithersburg, MD). The neutron wavelength was 0.81 nm with a full width at half-maximum (fwhm) spread of 0.11. Two sample-to-detector distances (1.50 and 15.30 m) were selected, covering an effective $\mathbf{Q}$ range between 0.002 and 0.3 Å^{-1}. A detector offset of 20 cm was employed

to provide adequate overlap for combining data sets. Ambient background and empty cell scattering were subtracted from the 2-D raw data. The corrected data were then circularly averaged to yield a 1-D intensity distribution, $I(\mathbf{Q})$, which was put on an absolute scale (cross section per unit volume) using the incident neutron flux. The incoherent scattering was obtained from the intensity plateau at high **Q** of the reduced data and was subtracted from the raw data. All of the SANS experiments were carried out at 30 °C.

Dynamic Light Scattering

Theory. For a dilute solution of monodisperse, noninteracting spherical particles, the Stokes−Einstein equation adequately describes the relationship between the particle's diameter d and the diffusion coefficient D and is written as

$$D = \frac{k_B T}{3\pi\eta d} \tag{2}$$

where k_B, T and η are the Boltzmann constant, absolute temperature, and solvent viscosity (D_2O, in our case), respectively.

The autocorrelation function (ACF), $G(\tau)$, obtained from the scattering data can be written as follows:

$$G(\tau) = \int_0^\infty I(t)\, I(t+\tau)\, \mathrm{d}t \tag{3}$$

where $I(t)$ is the detected intensity at time t and τ is the delay time. Assuming that the intensity distribution of the measured signal is Gaussian, we can rewrite the ACF as

$$G(\tau) = 1 + \gamma g(\tau)^2 \tag{4}$$

where $g(\tau)$ is the field autocorrelation function that can be expressed as the superposition of the different decaying modes

$$g(\tau) = \sum_i A_i \mathrm{e}^{-\Gamma_i \tau} \tag{5}$$

with the decay rate being

$$\Gamma_i = D_i \mathbf{Q}^2 \tag{6}$$

where **Q** is the scattering vector and A_i represents the prefactor of the ith mode. The data were reduced using CONTIN,[49] a cumulant analysis and regularization method with an inverse Laplace transformation. CONTIN calculates diffusion coefficients D_i by solving eq 5 through eigenvalue decomposition and uses a nonlinear statistical "smoothing" algorithm to reduce the number of parameters used to describe the data. CONTIN can be applied to both unimodal and multimodal size distributions.

Experiment. DLS experiments were performed on a Beckman N4 Plus photon correlation spectrometer at a scattering angle of 90°. The instrument is equipped with a laser source of wavelength 632.8 nm and an 80-channel correlator with multi-τ channel spacing. Before experimentation, the instrument was calibrated using a standard latex solution. All samples were tested at three different temperatures, 10 , 30 , and 50 °C. The viscosities at these temperatures are 1.679, 0.9759 and 0.6519, respectively. At comparable temperatures, solutions with D_2O, compared to those with H_2O, exhibit a higher viscosity due to increased hydrogen bonding. Both intensity- and number-weighted results were obtained. For quantitative comparisons of DLS results with SANS data, only number-weighted average histograms are shown in the paper. However, intensity-weighted histograms are better suited in distinguishing large particles such as MLV.

Results

Visual Observations. All ULV solutions were transparent with some "bluish" appearance, commonly seen in mixtures of vesicles with diameters in the range of tens of nanometers. The non-DMPG stock solution of $C_{lp} = 5.0$ wt % became opaque as the temperature increased from 4 to 25 °C and vice versa, presumably because of a transition from bicelles to MLV.[24] At high concentrations and low T (~10 °C), the nondoped lipid mixtures formed bicelles. Because of the small size of this structure, bicellar solutions are also transparent. However, MLV solutions usually appear opaque, and over a period of time, MLV colloids can separate macroscopically from solution. The 60/2/15 DMPC/DMPG/DHPC stock solution (also 5 wt %) remained transparent and became highly viscous when T was increased from 4 to 25 °C.

After mixing the two stock solutions to yield the desired DMPC/DMPG ratios, we stored the mixture at 4 °C for 1 day and then diluted it to 1.00 wt %. After a single freeze/thaw cycle, all 1.00 wt % solutions became totally transparent around 10 °C. When these samples (1 wt %) were heated to room temperature, their appearance turned from transparent, to bluish, and, finally, to opaque, indicative of a bicelle−ULV−MLV phase transition. These low NaCl solutions (<2 wt %) were stable only at low temperature for days, whereas mixtures with very high amounts of NaCl (10 wt %) remained clear for at least 6 months at 4 °C. The addition of NaCl can induce phase separation, resulting in an opaque appearance at room temperature; a similar change has also been observed in surfactant systems.[5] Though the appearance of the solution was used as a subjective determinant of MLV formation,[23,24,26] DLS intensity-weighted histograms have indicated the presence of a multimodal distribution with large particles (>100 nm).

All ULV samples were prepared by directly diluting the 1.00 wt % transparent solutions (bicelle phase) with D_2O at room temperature, the exception being the 0.033 wt % sample that was diluted from a 0.10 wt % sample at room temperature. Samples at 4 °C were subjected to a T jump and underwent a bicelle-to-vesicle transition[25] with an accompanying change of appearance, from clear to bluish, that remained unchanged for months at 4 °C. No phase separation was observed in samples with C_{lp} lower than 0.5 wt % and C_s lower than 0.33 wt % for 4 months. Phase separation occurred after only days or weeks in samples with $C_{lp} > 0.5$ wt % and $C_s > 0.33$ wt %. Slight cloudiness was observed in samples with C_{lp} higher than 0.33 wt % after a 4-month storage period in a refrigerator but was easily eliminated by shaking or heating the samples to room temperature. A similar observation was previously reported in CTAB/SOS surfactant systems.[6] A 2-D schematic phase diagram is presented in Figure 1 summarizing the various observations described.

Effects of C_{lp} and C_s on Vesicle Stability and Size. To study the effect of C_{lp} on the resultant self-assembled structures present in the various mixtures, we measured ULV size at a series of C_{lp} concentrations: 0.033, 0.10, 0.33, 0.50, and 0.75 wt % with $C_s = 0.1$ wt %. As mentioned previously, SANS experiments were conducted at 30 °C after the samples were incubated at 4 °C for a period of 1 month. DLS experiments were conducted at 10 , 30 , and 50 °C immediately after sample preparation and at intervals during the 4 months of storage, the only exception being the 0.75 wt % sample that turned opaque at T

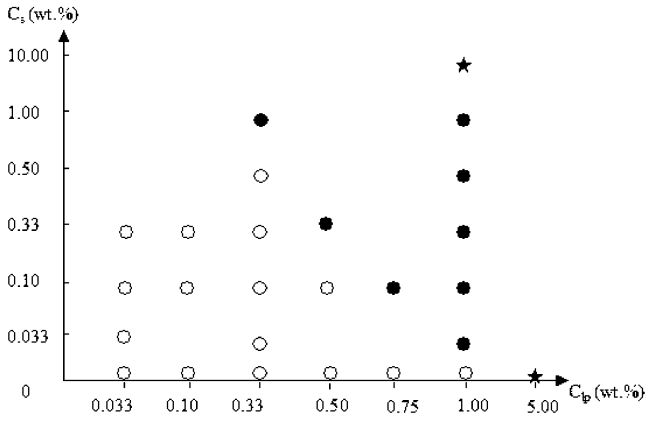

Figure 1. Schematic diagram of sample appearance as a function of C_{lp} and C_s: ○, transparent bluish tinge after prolonged storage at high and low temperatures; ●, transparent only at low T for a short period of time; ★, transparent and stable only at low T, but for an extended period of time.

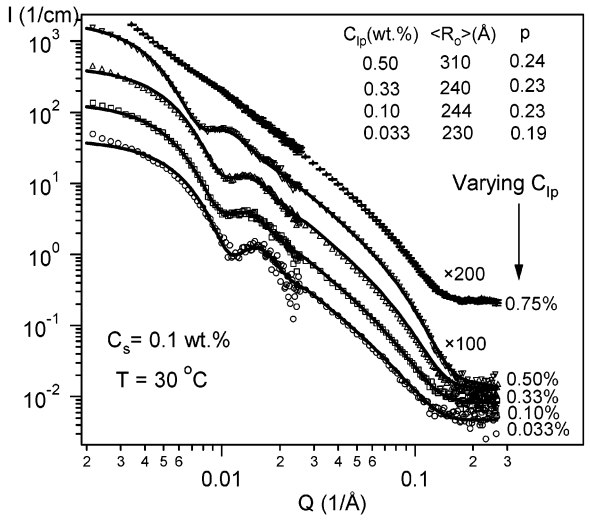

Figure 2. SANS data and fitting results for various C_{lp} values and a C_s of 0.10 wt %: C_{lp} = 0.033, 0.10, 0.33, 0.50, and 0.75 wt %, respectively. To better compare, scaling factors of 100 and 200 were applied to the 0.50 and 0.75 wt % data, respectively. An obvious size increase was observed when the C_{lp} reached 0.50 wt %. The data of the C_{lp} = 0.75 wt % sample were not fit because of the large object size and high polydispersity.

> 30 °C. The 0.75 wt % sample was tested only at 10 °C immediately after preparation.

SANS data and the corresponding best-fit curves using the three-parameter spherical shell model are presented in Figure 2. A detailed mathematical expression of the model has been described elsewhere.[23,24,26] For better comparison, the SANS data for the 0.50 and 0.75 wt % samples were offset by scaling factors of 100 and 200, respectively. The best-fit results from the spherical shell model are found to be in good agreement with the experimental data for $C_{lp} \leq 0.5$ wt % samples. The results also indicate that, as a function of C_{lp}, bilayer thickness (~3.2 nm) remains unaltered and in agreement with previously reported values.[23−26] Moreover, vesicle radii remain virtually constant (24 ± 1 nm) and are independent of lipid concentration for $C_{lp} \leq 0.33$ wt % samples. Larger monodisperse ULV (~31 nm) are observed for the C_{lp} = 0.5 wt % sample. For C_{lp} = 0.75 wt %, SANS data show a monotonic decay in intensity with a slope of −2, implying the existence of large, polydisperse aggregates, possibly large ULV.

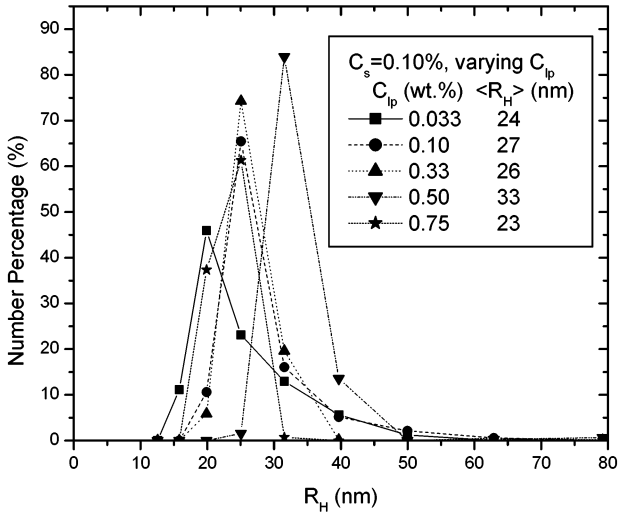

Figure 3. DLS size distribution functions for various C_{lp} (0.033, 0.10, 0.33, 0.50 and 0.75 wt %) at a fixed C_s (0.10 wt %). $\langle R_H \rangle$ values are similar for the three low concentrations (0.033, 0.10, and 0.33%) but shifted to larger size for the 0.50 wt % sample. Note that all of the data shown above were taken after 1 month of storage time except for the 0.75% sample, which was tested at 10 °C immediately after preparation to avoid phase separation.

DLS measurements (Figure 3) for $C_{lp} \leq 0.33$ wt % samples depict a unimodal size distribution of low polydispersity and a number-weighted average hydrodynamic radius, R_H, of about 25 ± 2 nm. Of note is that the best-fit vesicle radius from SANS experiments is usually slightly smaller than the hydrodynamic radius (R_H) measured by DLS. This is possibly due to the fact that R_H includes the contribution from associated water molecules whereas the radius obtained from SANS studies does not. Both SANS and DLS results demonstrate that the size of ULV remains practically unchanged over a range of C_{lp} (≤0.33 wt %). As C_{lp} was increased to 0.5 wt %, ULV size was found to increase. A clear bimodal distribution has been observed in the intensity-weighted histogram (not shown) for a C_{lp} = 0.75 wt % sample, indicating the presence of large aggregates. Although highly stable ULV were found when doped either with a charged lipid (i.e., DMPG) or a salt (i.e., $CaCl_2$),[25,26] this is the first observation of a highly stable ULV system doped simultaneously with a charged lipid (DMPG) and a salt (NaCl).

To study the effect of ionic strength, we added NaCl to liposomal solutions. Unlike Ca^{2+}, which strongly binds to lipid bilayers and, in some cases, induces vesicle fusion,[50] sodium salts such as NaCl and NaBr do not bind tenaciously to the lipid's headgroup. They can thus be used to control the ionic strength in surfactant and liposomal systems efficiently.[46,47,51] The effect of ionic strength on vesicles was tested by using samples prepared at three C_{lp} values: 0.033, 0.1, and 0.33 wt %. For the C_{lp} = 0.33 wt % sample, five salt concentrations (C_s = 0, 0.10, 0.33, 0.50, and 1.00 wt %) were examined, whereas only two C_s samples (0.10 and 0.33 wt %) were studied for the other C_{lp}.

Figure 4a and b depict SANS data for the above-mentioned samples. With the exception of the lowest (0 wt %) and highest (1 wt %) C_s, the best fits from SANS data yield a radius of 24 ± 1 nm and a polydispersity of ~20%. The sample with C_s = 0 wt % (non-NaCl-doped) had a slightly smaller radius (~20 nm) and also a slightly higher polydispersity (~30%); the sample with the highest C_s (1.00 wt %) turned opaque 1 day after preparation, presumably forming MLV.

The finding of forming nearly constant-size ULV was also examined by DLS. Figure 5a and b shows the size distributions

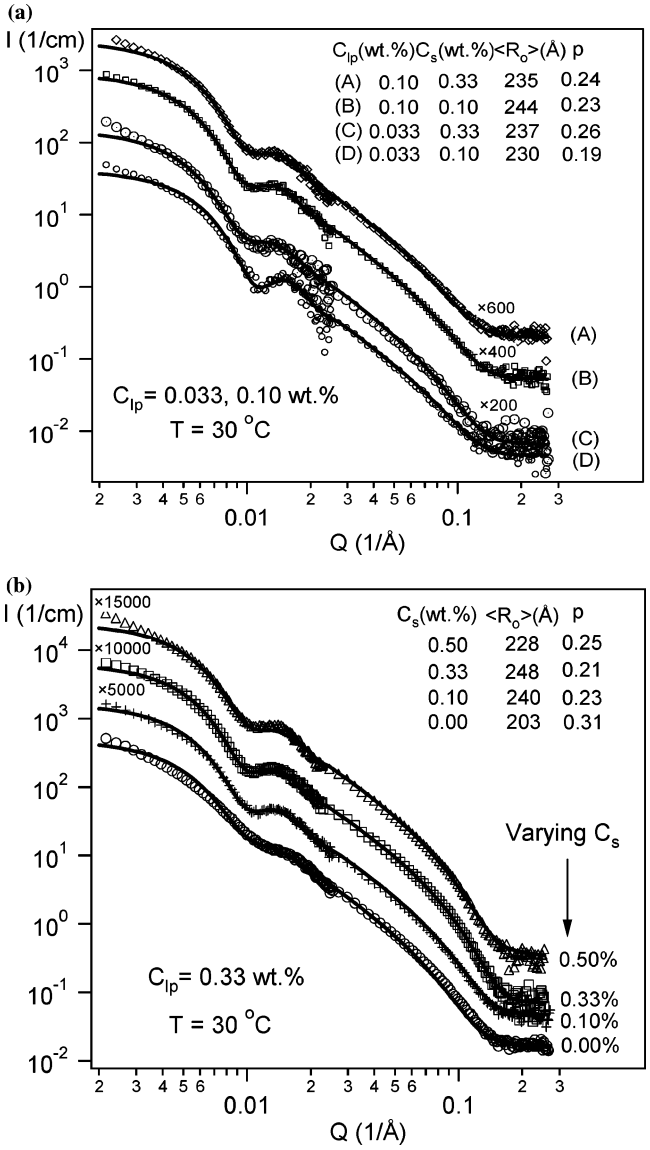

Figure 4. SANS data and best-fit results for samples with various C_s at (a) C_{lp} = 0.033, 0.10 wt % and (b) C_{lp} = 0.33 wt %. Two salt concentrations (C_s = 0.1 and 0.33 wt %) were investigated for samples with C_{lp} = 0.033 and 0.10 wt %, whereas four C_s values (0, 0.1, 0.33, and 0.5 wt %) were examined for the samples with C_{lp} = 0.33 wt %. Data were rescaled to better compare. Vesicle radii were found to be nearly constant except for the sample without NaCl (C_s = 0 wt %), where the radius was smaller.

obtained from DLS that exhibited similar histograms for all samples. Though the polydispersity of the samples varied with salt and lipid concentrations, it is shown that all number-weighted $\langle R_H \rangle$ values were around 25 ± 3 nm, except for the C_s = 0% sample, whose $\langle R_H \rangle$ is 16 nm. From an intensity-weighted size distribution analysis, we found another small peak with a much larger R_H (>100 nm) in a few samples. Their negligible number percentages were not seen in the number-weighted histograms. The existence of a few large particles may explain the discrepancy between the SANS data and the fit to the data at very low **Q** values (<0.04 nm^{-1}).

Other Effects on Vesicle Stability and Size. *Time Evolution.* The stability of ULV size versus time for four different C_{lp} samples (0.033, 0.1, 0.33, and 0.5 wt %) was monitored using DLS. All samples were kept at 4 °C for the first 4 months before experimentation. DLS measurements were taken immediately after the temperature was increased to 30 °C. Table 1 depicts

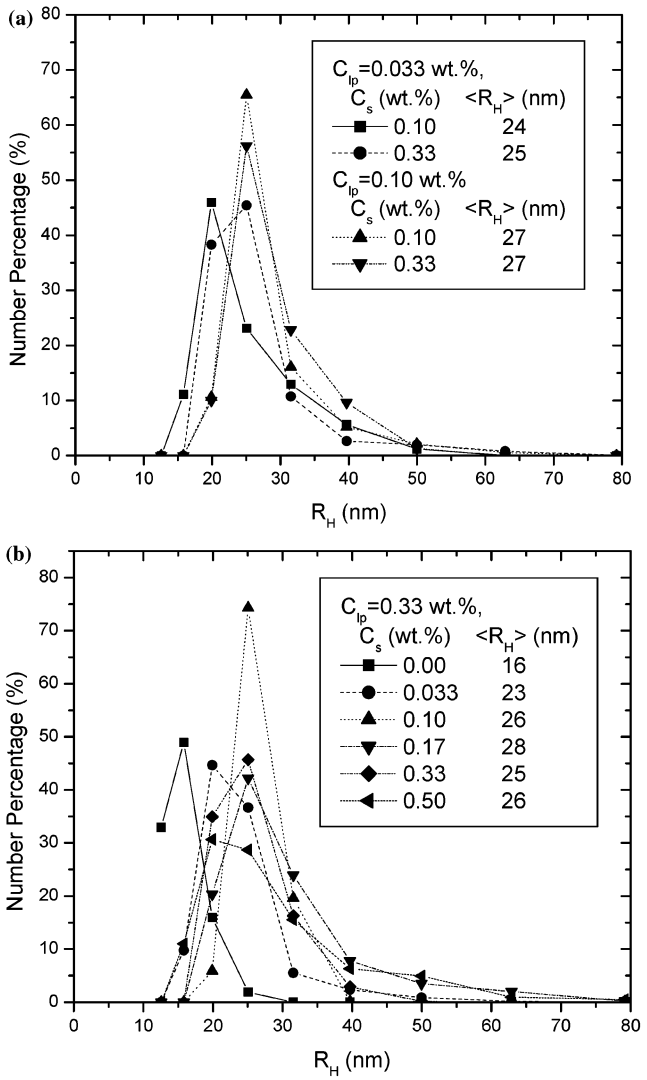

Figure 5. Size distribution functions under different salt concentrations and lipid concentrations: (a) C_{lp} = 0.033 and 0.10 wt % and (b) C_{lp} = 0.33 wt %. Monodisperse vesicles with nearly constant size were observed for all samples except for the one with C_s = 0 in b, where the vesicle size is smaller.

TABLE 1: Number-Weighted Average Hydrodynamic Radius $\langle R_H \rangle$ (nm) Obtained from Four Selected Samples versus Time after the DLS Measurements Were Taken[a]

C_{lp}, C_s (wt %)	0 month	1 month	2 months	4 months	5 months
0.033, 0.33	26	25	26	27	25
0.10, 0.10	25	27	X	X	28
0.33, 0.33	24	25	24	27	28
0.50, 0.10	34	33	X	X	X

[a] In general, the ULV size increases very slightly over the period of testing.

the evolution of the number-average $\langle R_H \rangle$ of four samples over a 4-month period. For $C_{lp} \leq$ 0.1 wt %, $\langle R_H \rangle$ values of ULV were found to be practically invariant over the 4-month storage period at 4 °C, in addition to 1 month of storage at 30 °C. For the most part, ULV size remains practically unchanged. The C_{lp}/C_s = 0.50/0.1% sample became unstable after 2 months of storage and had phase separated. Figure 6 shows the size evolution of a C_{lp}/C_s = 0.33/0.33% mixture, exhibiting a narrow unimodal distribution immediately after sample preparation. The appearance of the sample remained unchanged during the first 4 months but became cloudy after 1 month of storage at 30 °C. In this case, another peak (>100 nm) is observed in the intensity

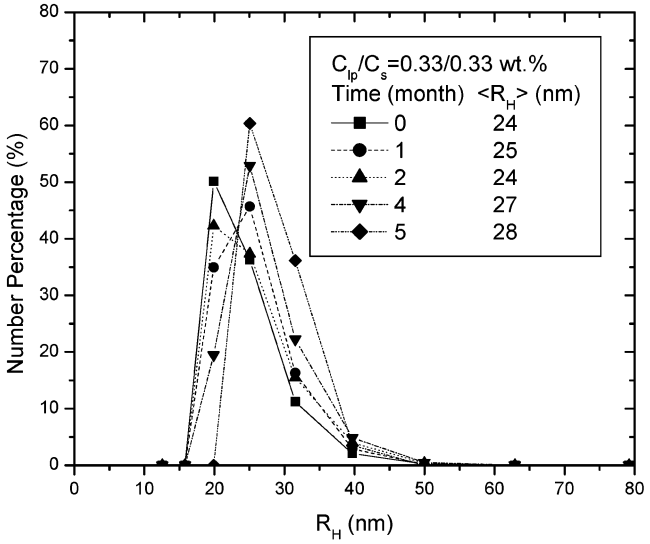

Figure 6. Size evolution as a function of time for the 0.33/0.33 wt % sample. A slight increase was observed after 5 months.

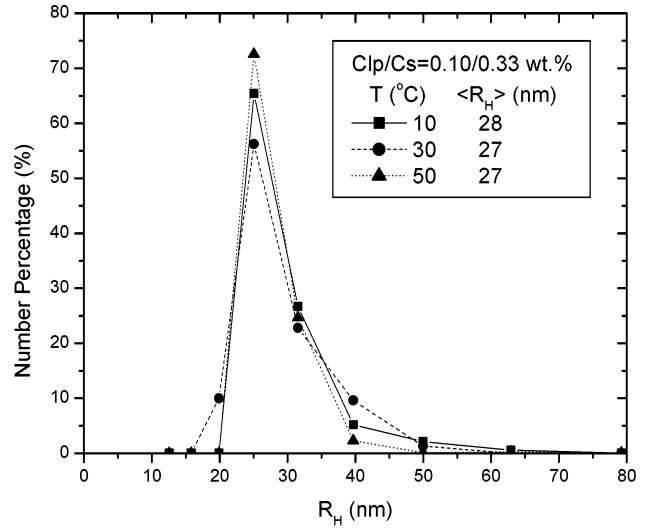

Figure 7. Size distribution for a $C_{lp} = 0.10$ and $C_s = 0.33$ wt % sample at 10 , 30 , and 50 °C. The data show that as a function of temperature the ULV size remains practically unaltered.

histogram (not shown), indicative of the formation of large aggregates, possibly MLV.

Effect of Temperature. The structural phase transition of DMPC/DHPC mixtures is often observed when the temperature is increased beyond the chain-melting transition of DMPC, around 23 °C.[23,24] Within the range of C_{lp} investigated (<1 wt %), most of the structures formed above T_M were structures with a higher curvature (e.g., ULV), in contrast to bicelles, which are found at temperatures below T_M. An exception to this is certain DMPC/DHPC mixtures that form ULV both above and below T_M.[25,26] This may imply that changes to DMPC's hydrocarbon chain conformation may not directly affect the self-assembled structure.

In the present study, ULV stability as a function of temperature was examined via DLS for samples prepared at three lipid concentrations. Figure 7 shows the size distribution for a C_{lp}/C_s = 0.1/0.33 wt % sample at 10, 30, and 50 °C. Size distributions are practically indistinguishable and appear to be narrow at higher temperatures. A similar behavior has been observed in the $C_{lp} = 0.33$ wt % sample; however, the $C_{lp} =$ 0.75 wt % sample became opaque at $T > 25$ °C, indicating the presence of MLV.

Discussion

Effect of Lipid Concentration, C_{lp}. The size of spontaneously forming ULV, in general, varies with C_{lp}.[25,26] Our observations of samples with $C_{lp} > 0.33$ wt % are consistent with those previously reported. For cases of $C_{lp} \leq 0.33$ wt %, the vesicle size becomes C_{lp}-independent, similar to that for systems doped with either DMPG or Ca^{2+} ions but not with both.[25,26] A previous study of nondoped ([DMPC]/[DMPG] = ∞) and strongly DMPG-doped ([DMPC]/[DMPG] = 15) systems, at the same temperature and lipid concentration, confirmed the presence of MLV and bicelles, respectively.[24] MLV are vesicles composed of a wide range of radii and conformations, which are entropically stabilized and incur only a small penalty for deviating from their spontaneous curvature. The formation of bicelle systems with elevated DMPG levels implies that strong Coulombic interactions between charged lipids may stiffen the membrane and drive the short-chain DHPC lipids toward the rim of the disklike bicellar structure. When introduced with an appropriate amount of charge, DMPC/DHPC mixtures form a vesicular structure with a specific radius (possibly related to the spontaneous curvature of the system). This implies that an appropriate surface charge may induce a reasonably deep local free-energy minimum resulting in the observed size insensitivity. Note that the ratio between charged (DMPG) and noncharged lipids was held constant during the entire study, with the assumption that the ULV membrane composition remains unaltered as a function of temperature and concentration. The size insensitivity to lipid concentration also contradicts the predictions by Oberdisse et al.,[39,40] whose results, for a given surface charge density, indicate a size increase with increasing lipid concentration. In our experiments, the range of total lipid concentration, whereby ULV radii remained unaltered, was small (<0.5 wt %) and even smaller for the case of charge density. The insensitivity of ULV to a changing chemical potential may be the result of a deep local free energy in forming the self-assembled structures.

Recently, Leng, Egelhaaf, and Cates[47] proposed a kinetic model to explain the formation of vesicles in a lecithin/bile salt system. The model stated that ULV can be kinetically trapped as the detergent (charged short-chain lipid) molecules are removed from the rim of disklike micelles (bicelles) upon dilution. In the Leng et al.[46,47] study, bicelles coalesce into a larger planar structure to compensate for the loss of short-chain lipids. As the radius of the newly formed bicelles reaches a critical radius, r^*, the rate of vesicle formation exceeds the rate of forming larger bicelles, and most of the short-chain lipids (bile salt) are released from the bicelle's rim into the bulk solution. The vesicle size is, therefore, approximately equal to $r^*/2$, depending on the interaction between aggregates, packing constraints, and salt concentrations. Once vesicles are formed, the size may be insensitive to certain changes in salt or lipid concentration because only a small amount of bile salt remains in the membranes. The formation of ULV in our study is different from the scenario just described. Although bicelles were found at $C_{lp} = 1$ wt % and low temperature,[26] the short-chain DHPC lipid does not carry any charge and most likely localizes itself at the rim of the bicelle. Most of the charged DMPG molecules are expected to stay in the bilayers with DMPC because both compounds have the same chain length. This, of course, does not preclude the formation of ULV from another kinetically controlled mechanism. However, more

studies on the stability and the size of ULV formed via various pathways are needed.

Effect of Ionic Strength. The screening effect of Coulombic interactions on the self-assembled charged structures can be studied by changing the ionic strength (e.g., salt concentrations) of the solution and thus the Debye length, χ_D. Our experimental results show a slightly smaller vesicle radius for the NaCl-free mixtures (~20 nm, SANS) compared to that for mixtures with NaCl (~24 nm, SANS). Assuming complete dissociation of DMPG in a NaCl-free mixture with $C_{lp} = 0.33$ wt %, the calculated χ_D is about 38.5 nm, larger than the radius of curvature. The surface charge density of a DMPC/DMPG bilayer (neglecting the charge difference between the inner and outer layers and taking $R_o = 24$ nm and $R_i = 21$ nm) is about 3.5×10^{-3} C/m^2. Compared to calculations by Winterhalter and Helfrich,[30,31] the above experimental charge density and Debye length decrease and result in a small, positive bending modulus and a negative Gaussian modulus, leading to a negative total elastic energy favoring spontaneous vesiculation. Reducing the screening length (by increasing salt concentration) reduces the bending modulus; however, under the present charge density conditions, the negative Gaussian modulus *increases* with ionic strength, eventually leading to a positive total energy at a threshold $C_{s,MLV}$ value, where the transition from ULV to MLV takes place.

Figure 1 depicts such a trend as a function of salt concentration. An increase in vesicular size (from 20 to 24 nm according to SANS data) upon the addition of NaCl agrees with the above explanation. For samples doped with NaCl, the Debye length χ_D varies from 4 nm ($C_s = 0.033$ wt %, 5.6 mM) to 1.3 nm ($C_s = 0.33$ wt %, 56 mM), with the ULV size remaining unaltered. Again, our observations of ULV size insensitivity are in contradiction to what has been predicted by Oberdisse et al.[39,40] In their case, the size monotonically increased with salinity at higher charge density. Though there is no direct comparison between our data and calculations from a more detailed treatment, such as P-B theory with translational entropy, asymmetric charge density, and so forth, the insensitivity of vesicular size may be attributed to a low entropic contribution due to low lipid concentration and a dominant enthalpic contribution. As the lipid concentration increases, other degrees of freedom should be considered, and the entropic contribution should increase with the total lipid concentration, eventually destabilizing the ULV structure at a threshold salinity of $C_{s,MLV}$, which decreases with total lipid concentration (as shown in Figure 1). A more extensive study is presently in progress to better understand the various structures and their stability at present lipid and salt concentrations.

Aging and Temperature Effect. The size evolution of ULV systems depends on the rate of exchange between the surfactant/lipid from aggregates to solution and the flip-flop rate of surfactant/lipid molecules between the inner and outer leaflets. Although it was found that the size of certain surfactant vesicles remained unaffected over a period of months,[52] sometimes vesicle size was observed to increase rapidly over a short period of time and then slowly stabilize over a period of months.[53] Nonsterically stabilized lipid vesicles are rarely stable for extended periods.[14,15]

Despite an invariant ULV size (Figure 6), the issue of whether these ULV are kinetically trapped or thermodynamically stable is not yet understood. After 4 months, a slight increase in size and polydispersity was observed in the $C_{lp} = 0.33$ wt % sample, implying either a slow structural evolution or lipid degradation. Note that samples were stored at 4 °C, lower than the T_M of DMPC, except during measurements. For the most part, DMPC was in the gel phase, a more rigid molecular structure than the L_α phase, hence the exchange rate of DMPC from ULV to solution or vice versa was slow. The invariant ULV size at low temperature (4 °C) may suggest that ULV are kinetically trapped. After 4 months of storage at 4 °C, the $C_{lp} = 0.33$ wt % sample was heated to 30 °C and incubated for a period of 1 month. After incubation, the sample was studied with DLS, indicating the possible presence of MLV.

Conclusions

Low-polydispersity, spontaneously forming ULV were found in DMPC/DMPG/DHPC phospholipid mixtures by diluting a high-concentration lipid solution at low temperature (4 °C). SANS and DLS results show that the ULV are reasonably stable over extended periods of time and are unaffected by certain changes in lipid concentration, solution ionic strength, and temperature. Under the imposed constant surface charge density, the structural phase diagram could be explained by the theoretical predictions of Winterhalter and Helfrich.[30,31] However, the nearly constant ULV size as a function of lipid concentration ($C_{lp} < 0.33\%$), salinity ($C_s < 0.5$ wt %), and temperature is different from theoretical predictions[39,40] and previous experimental reports. A possible explanation may be that the enthalpic contribution from the negative Gaussian modulus dominates at low lipid concentrations. Another possibility may be the energetically favorable packing of DMPC and DMPG that renders a slow response to changes in chemical potential and structural transformation at low concentrations. Further work on stable structures obtained via various pathways in systems with the same chemical composition is needed to understand the formation mechanism of these ULV. Such an understanding may then facilitate the design of ULV for prolonged stability and encapsulation needed for pharmaceutical and biomedical applications.

Acknowledgment. We thank the instrument scientists at NCNR NG7 for their assistance. C.-Y.H. is grateful for the financial support of the SBR grant from NJIT. J.K. and M.-P.N. are grateful for funding from the Advanced Foods and Materials network in Canada. Also, we acknowledge an insightful discussion with Dr. V. A. Rughunathan (Raman Research Institute).

References and Notes

(1) Kaler, E. W.; Murthy, A. K.; Rodrigues, B. E.; Zasadzinski, J. A. *Science* **1989**, *245*, 1371.
(2) Kaler, E. W.; Herrington, K. L.; Murthy, A. K.; Zasadzinski, J. A. *J. Phys. Chem.* **1992**, *96*, 6698.
(3) Murthy, A. K.; Kaler, E. W.; Zasadzinski, J. A. *J. Colloid Interface Sci.* **1991**, *145*, 598.
(4) Hoffmann, H.; Thunig, C.; Munkert, U. *Langmuir* **1992**, *8*, 2629.
(5) Hoffmann, H.; Munkert, U.; Thunig, C.; Valinente, M. *J. Colloid Interface Sci.* **1994**, *163*, 217.
(6) Yatcilla, M. T.; Herrington, K. L.; Brasher, L. L.; Kaler, E. W.; Chiruvolu, S.; Zasadzinski, J. A. *J. Phys. Chem.* **1996**, *100*, 5874.
(7) Bergström, M. *Langmuir* **1996**, *12*, 2454.
(8) Bergström, M.; Eriksson, J. C. *Langmuir* **1996**, *12*, 624.
(9) Bergström, M.; Eriksson, J. C. *Langmuir* **1998**, *14*, 288.
(10) Bergström, M.; Pedersen, J. S.; Schurtenberg, P.; Egelhaaf, S. U. *J. Phys. Chem. B* **1999**, *103*, 9888.
(11) Bergström, M.; Pedersen, J. S. *J. Phys. Chem. B* **2000**, *104*, 4155.
(12) Bergström, M. *J. Colloid Interface Sci.* **2001**, *240*, 294.
(13) Viseu, M. I.; Edwards, K.; Campos, C. S.; Costa, S. M. *Langmuir* **2000**, *16*, 2105.
(14) Lasic, D. *TIBTECH* **1998**, *16*, 307.
(15) Lasic, D. D.; Joannic, R.; Keller, B. C.; Frederik, P. M.; Auvray, L. *Adv. Colloid Sci.* **2001**, *89*−*90*, 337.
(16) Gabriel, N. E.; Roberts, M. F. *Biochemistry* **1984**, *23*, 4011.

(17) Ollivon, M.; Lesieur; S.; Grabrielle-Madelmont, C.; Paternotre, M. *Biochim. Biophys. Acta* **2000**, *1508*, 34.
(18) Schurtenberger, P.; Mazer, N.; Waldvogel, S.; Kanzig, W. *Biochim. Biophys. Acta* **1984**, *775*, 111.
(19) Schurtenberger, P.; Mazer, N.; Kanzig, W. *J. Phys. Chem.* **1985**, *89*, 1042.
(20) Egelhaaf, S. U.; Schurtenberger, P. *Phys. Rev. Lett.* **1999**, *82*, 2804.
(21) Andelman, D.; Kozlov, M. M.; Helfrich, W. *Europhys. Lett.* **1994**, *25*, 231.
(22) Lesieur, P.; Kiselev, M. A.; Barsukov, L. I.; Lombardo, D. *J. Appl. Crystallogr*. **2000**, *33*, 623.
(23) Nieh, M.-P.; Glinka, C. J.; Krueger, S.; Prosser, R. S.; Katsaras, J. *Langmuir* **2001**, *17*, 2629.
(24) Nieh, M.-P.; Glinka, C. J.; Krueger, S.; Prosser, R. S.; Katsaras, J. *Biophys. J.* **2002**, *82*, 2487.
(25) Nieh, M.-P.; Harroun, T. A.; Raghunathan, V. A.; Glinka, C. J.; Katsaras, J. *Phys. Rev. Lett.* **2003**, *91*, 158105.
(26) Nieh, M.-P.; Harroun, T. A.; Raghunathan, V. A.; Glinka, C. J.; Katsaras, J. *Biophys. J.* **2004**, *86*, 2615.
(27) Seelig, J.; MacDonald. P. M.; Scherer, P. G. *Biochemistry* **1987**, *26*, 7535.
(28) Kurland, R.; Newton, C.; Nir, S.; Papahadjopoulos, D. *Biochimica Biophys. Acta* **1979**, *551*, 137.
(29) Helfrich, W. Z. *Naturforsch.* **1973**, *28C*, 693−703.
(30) Winterhalter, M.; Helfrich W. *J. Phys. Chem.* **1988**, *92*, 6865.
(31) Winterhalter, M.; Helfrich W. *J. Phys. Chem.* **1992**, *96*, 327.
(32) Lekkerkerker, H. N. W. *Physica* **1989**, *A159*, 319.
(33) Lekkerkerker, H. N. W. *Physica* **1990**, *A167*, 384.
(34) Mitchell, D. J.; Ninham B. W. *Langmuir* **1989**, *5*, 1121.
(35) Kumaran, V. *Phys. Rev. E* **2001**, *64*, 051922.
(36) Safran, S. A.; Pincus, P.; Andelman, D.; Mackintosh, F. C. *Phys. Rev. A* **1991**, *43*, 1071.
(37) Safran, S. A.; Pincus, P.; Andelman, D. *Science* **1990**, *248*, 354.
(38) Oberdisse, J.; Couve, C.; Appell, J.; Berret, J. F.; Ligoure, C.; Porte, G. L*angmuir* **1996**, *12*, 1212.
(39) Oberdisse, J.; Porte, G. *Phys. Rev. E* **1997**, *56*, 1965.
(40) Oberdisse, J. *Eur. Phys. J. B* **1998**, *3*, 463.
(41) Israelachvili, J. N.; Mitchell, D. J.; Ninham, B. W. *Faraday Trans.* **1976**, *72*, 1525.
(42) Israelachvili, J. N.; Mitchell, D. J.; Ninham, B. W. *Biochim. Biophys. Acta* **1977**, *470*, 185.
(43) Nagarajan, R.; Ruckenstein, E. *J. Colloid Interface Sci.* **1979**, *71*, 580.
(44) Yuet, P. K.; Blankschtein, D. *Langmuir* **1996**, *12*, 3802.
(45) Yuet, P. K.; Blankschtein, D. *Langmuir* **1996**, *12*, 3819.
(46) Leng, J.; Egelhaaf, U.; Cates, M. E. *Europhys. Lett.* **2002**, *59*, 311.
(47) Leng, J.; Egelhaaf, U.; Cates, M. E. *Biophys. J.* **2003**, *85*, 1624.
(48) Hayter, J. B.; Penfold, J. *Molecular Phys.* **1981**, *42*, 109.
(49) Provencher, S. W. *Comput. Phys. Commun*. **1982**, *27*, 229.
(50) Koynova R.; Caffrey, M. *Biochim. Biophys. Acta* **1998**, *91*, 1376.
(51) Brasher, L. L.; Kaler, E. W. *Langmuir* **1996**, *12*, 6270.
(52) Marques, E. F. *Langmuir* **2000**, *16*, 4798.
(53) Iampietro, D. J.; Kaler, E. W. *Langmuir* **1999**, *15*, 8590.
(54) The identification of any commercial product or trade name does not imply endorsement or recommendation by the National Institute of Standards and Technology (NIST).